Desalination and Water Treatment
www.deswater.com

doi: 10.5004/dwt.2018.22649

123 (2018) 150–155
August

Adsorption behavior of poly(methacrylic acid)/iron-oxide-coated zeolite for the removal of Mn(II), Fe(II), and As(III) from aqueous solution

Seo-Hyun Pak[a], Seung-Min Park[a], Jusuk An[a,b], Chan-gyu Park[a,*]

[a]*Environmental Technology Division, Korea Testing Laboratory, 87, Digital-ro 26-gil, Guro-gu, Seoul 08389, Korea, Tel. +82 2-860-1105, +82 2-860-1272; Fax: +82 2-860-1689; email: pcg6189@hotmail.com (C.-g. Park), Tel. +82 2-860-1139; Fax: +82 2-860-1689; email: seohyunpak@ktl.re.kr (S.-H. Pak), Tel. +82 2-860-1593; Fax: +82 2-860-1689; email: jrpeter@ktl.re.kr (S.-M. Park), Tel. +82 2-860-1183; Fax: +82 2-860-1689; email: jusuk@ktl.re.kr (J. An)*
[b] *School of Civil and Environmental Engineering, Yonsei University, Seoul, Korea*

Received 22 November 2017; Accepted 17 June 2018

ABSTRACT

Polymer-modified zeolite has the potential to combine the advantages of polymers and zeolites while overcoming the drawbacks of both materials. In this study, a zeolite modified with poly(methacrylic acid) and iron-oxide (MA-zeolite) was successfully prepared using the graft polymerization method. The MA-zeolite was synthesized from clinoptilolite. The MA-zeolite was characterized and applied for the removal of Mn(II), Fe(II), and As(III) from aqueous solutions. Brunauer–Emmett–Teller surface areas, scanning electron microscopy, and Fourier transform infrared spectroscopy were used to study the surface properties of the MA-zeolite. The adsorption ability of the zeolite modified with poly(methacrylic acid) toward metals and metalloids such as Mn(II), Fe(II), and As(III) was studied and the results compared with those for raw zeolite and iron-oxide-coated zeolite. The MA-zeolite showed good adsorption ability, and the removal percentages decreased from Fe(II), Mn(II), to As(III).

Keywords: Grafting polymerization; Modification; Zeolite; Water treatment; Manganese; Iron; Arsenic

1. Introduction

Exposure to excessive amounts of heavy metals is harmful to human beings, other animals, and plants [1,2]. Most often, the definition of toxic metals includes, at least, *cadmium*, *manganese*, *lead*, *mercury*, and iron. These metals have rapidly become significant environmental pollutants with increasing industrial wastewater emission. Therefore, the treatment of heavy metals in wastewater has become crucial.

Until now, various treatment methods to remove toxic pollutants (metals and metalloids) from wastewater such as microfiltration [3], ultrafiltration [4], nanofiltration [5], adsorption (activated carbon), and ion-exchange [6] have been widely investigated and developed. However, they have serious drawbacks, such as ineffectiveness, high cost, and the production of secondary pollutants [7]. Many researchers have tried to solve these problems by developing effective, cheap adsorbents. Examples of such adsorbents are zeolites, peat moss, and clay.

Natural zeolite is a crystalline aluminosilicate consisting of a skeleton of tetrahedral molecules and has many advantages such as unique activity, highly crystalline structure, high adsorption capability, low cost, and good adsorption of heavy metals, nitrates, phosphates, and organic pollutants from wastewater [8]. However, the adsorption ability of zeolites toward heavy metals is lower than those of other adsorbents, and zeolites tend to aggregate during adsorption in wastewater. To overcome these limitations, the modification of zeolites by chemical reactions, polymerization, and with metal oxides has been carried out to increase their adsorption efficiency.

Calvo et al. [9] studied a zeolite modified with hexadecyltrimethylammonium bromide. This modification improves the anion exchange properties of the zeolite. Barloková et al. [10]

* Corresponding author.

reported an efficient route to modify zeolites with iron hydroxides, which enhance the sorption capacity of natural zeolite for heavy metal ions. However, methods for metal modification are complex, and the removal efficiency is significantly lowered by the selective adsorption of negative charge [11].

Recently, various polymers with hosts such as zeolite and mesoporous materials have received attention as adsorbents for the removal of heavy metals. Roque et al. [12] studied pyrrole oligomerization within zeolite channels. Densakulprasert et al. [13] reported various polyaniline-zeolite (Y, 13X, and A1MCM-41) composite systems that act as sensors for CO and N_2 gas. Im et al. [14] studied the crystallization behavior and fine structure of poly(ethylene terephthalate)/A-zeolite nanocomposites. In this study, a synthetic route for polymerized zeolite has been designed, and the modified zeolite has been applied as an adsorbent. The iron-oxide-coated zeolite with graft polymerized poly(methacrylic acid) (MA-zeolite) was characterized by the Brunauer–Emmett–Teller (BET) surface area, scanning electron microscopy (SEM) images, Fourier transform infrared (FTIR), and the removal ability for iron, manganese, and arsenic ions from wastewater was studied. This study demonstrates the potential application of polymerized zeolite as an adsorbent.

2. Materials and methods

2.1. Chemicals and materials

The reagents used for the modification of iron-oxide-coated zeolite were purchased from Sigma-Aldrich (USA): methacrylic acid (MA), sodium persulfate ($Na_2S_2O_8$), and sodium metabisulfite ($Na_2S_2O_5$) were used without further purification. Mn(II)SO_4 and Fe(II)SO_4 were reagent grade and obtained from Samchun Chemical (Korea). Stock solutions of arsenite (As(III)) were prepared from As_2O_3 (Fluka, USA).

Natural zeolite (clinoptilolite) samples were used in the present investigation and supplied by Rex Material Co., Ltd in Pohang (Korea). The estimated cation exchange capacity of natural zeolite with respect to its formula ($Na_2CaAl_2SiO_{18}\cdot 6H_2O$) is 0.8–1.2 meq/g, as measured by the manufacturer.

2.2. Synthesis

2.2.1. Iron-oxide-coated zeolite

The zeolite (clinoptilolite) was stored at 105°C for 1 d before use. Then, 1 kg of zeolite was added to a 500-mL aqueous solution of 10% $FeCl_3$ (≥99.99%, Sigma-Aldrich) at pH 10 and mixed for 60 min at 150°C. Subsequently, the water was removed using a vacuum distiller. The remaining material was dried at room temperature for 2 h to produce iron-oxide-coated zeolite.

2.2.2. Graft polymerization procedure (MA-zeolite)

Methacrylic acid (5 mL, MA, monomer, 99%) was added to 95 mL deionized water in a beaker. Then, 1 mM $Na_2S_2O_8$ and 0.1 mM $Na_2S_2O_5$ were added. After dissolving the salts, the iron-oxide-coated zeolites were added to the above solution. The reaction mixture was treated at room temperature with shaking (200 rpm). After 15, 30, 60, or 120 min, the products were washed with deionized water. The modified zeolites were stored in deionized water for stabilization. The obtained samples were denoted as MA-zeolite (*x* min), where *x* is the treatment time at room temperature. The graft polymerization reaction is shown in Fig. 1. When a reagent such as $Na_2S_2O_5$ and $Na_2S_2O_8$ was added to a solute (ultrapure water) on the iron oxide surface, the salt solutions served as reaction initiators. Radicals such as $SO_4^{\bullet}$ and $S_2O_5^{\bullet}$ induce $OH^{\bullet}$, and the strong oxidizing power of $OH^{\bullet}$ leads to the disconnection of the double bond between the surface of the iron oxide and the inside of the cavity, eventually leading to instability (Fig. 1(b)).

When methacrylic acid is added, the surrounding ions and iron oxide surface are bound to each other inside the pores. This reaction was carried out for various periods, as shown in Fig. 1(c).

2.3. Batch sorption studies

Batch sorption experiments were carried out using 1 g of the adsorbent with 40 mL of metal solutions containing Mn(II), Fe(II), and As(III) ions of the desired concentrations at room temperatures in 50 mL conical tubes. All experiments

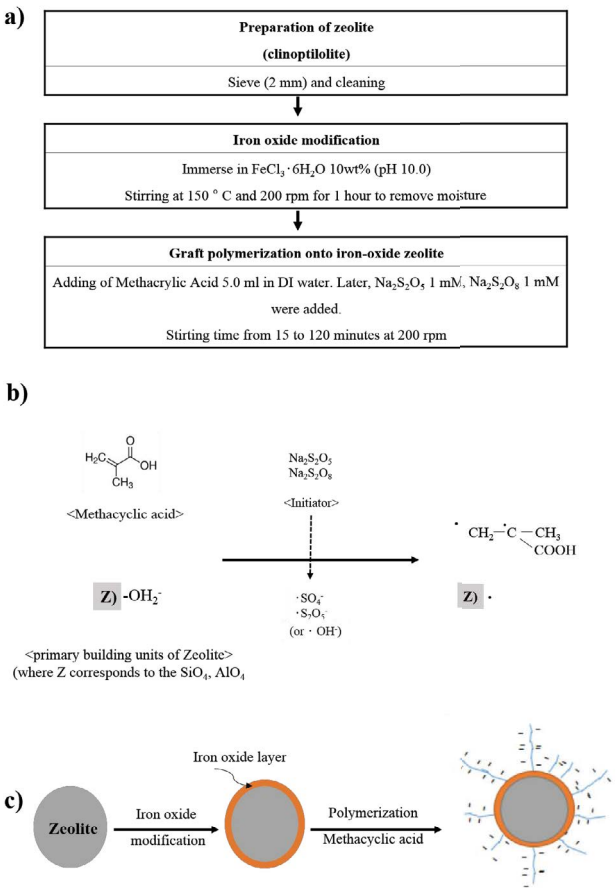

Fig. 1. (a) Surface modification of iron-oxide-coated zeolite: graft polymerization process, (b) activation of methacrylic acid and zeolite by an initiator, and (c) schematic diagram of graft polymerization.

were conducted with shaking at 200 rpm. The concentrations of the manganese and iron solutions were determined by UV/vis spectroscopy (Hach, DR 5000, USA) using standard methods (Mn: Periodate Oxidation Method/Fe: FerroVer® Method) for examining water. The concentration of arsenic was determined by inductively coupled plasma measurements (ICP, VARIAN 730ES, Australia).

2.4. Characterization

The organic functional groups were characterized by attenuated total reflection Fourier transform infrared spectroscopy (ATR-FTIR; Nicolet spectrophotometer 5700, ThermoElectron Corp., MA) with a ZnSe crystal at an incident angle of 45°. All spectra were recorded at 25°C and corrected for the atmospheric background spectra. SEM (S-4800, Hitachi, Japan) was used to verify the morphology. The samples were sputtered with a thin film of gold. The specific surface area was calculated using the BET method.

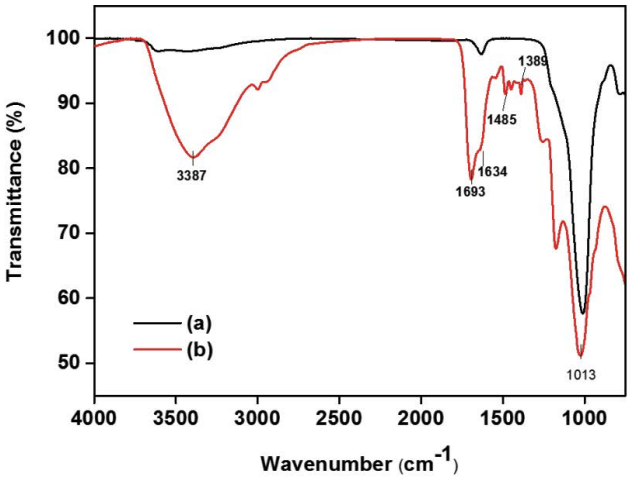

Fig. 2. ATR-FTIR spectra for the (a) raw zeolite and (b) zeolite modified with methacrylic acid (MA).

3. Results and discussion

3.1. Poly(methacrylic acid)/zeolite composite

The poly(methacrylic acid)/zeolite composite was obtained by treating the iron-oxide-coated zeolite with MA, and the product was evaluated for the adsorption of heavy metals. BET analysis was performed to determine the differences between the surface of raw zeolite and that of MA-zeolite. The surface area can be obtained by calculating the amount of adsorbed nitrogen gas on the powder surface using the BET equation. The surface area of MA-zeolite was 34 m^2/g, which is similar to the values obtained in other studies of modified zeolites [15]. In addition, it was confirmed that the surface area decreased from 40 to 34 m^2/g because of the reduction of the internal pore volume by graft polymerization.

ATR-FTIR was used to confirm the formation of amide bonds and the presence of certain functional groups on the iron-oxide-coated zeolite surface after each modification. The spectra were recorded in two regions: 4,000–2,800 cm^{-1}, where the characteristic bands of –OH, –NH, and –CH are located, and 1,800–1,100 cm^{-1}, where the absorption bands characteristic of the amide group are located.

The FTIR spectra of raw zeolite and MA-zeolite are shown in Figs. 2(a) and (b). The FTIR spectra of the polymerized sample (Fig. 2(b)) contain absorption bands at 1,693 and 3,387 cm^{-1}, which were not observed in the spectrum of raw zeolite [16].

The bands at 1,693 and 3,387 cm^{-1} arise from –C=O and –OH group stretching vibrations [15]. In addition, the bands at 1,634 and 1,389 cm^{-1} are characteristic of symmetric $\gamma_s(COO^-)$ and asymmetric $\gamma_{as}(COO^-)$ modes, respectively [17]. In addition, the peak at 1,485 cm^{-1} suggests $-CH_3$ stretching. The sharp peak around 1,013 cm^{-1} is indicative of the zeolite framework [18,19]. This peak may be a feature of zeolites that contain the hydrated triple crankshaft chains.

The surface morphologies of the iron-oxide and the graft copolymer coatings were observed by SEM. The SEM images of (a) raw zeolite and (b) iron-oxide-coated zeolite show the rough surfaces with irregularly shaped particles of various sizes. The SEM images of the grafted samples (Figs. 3(c)–(f)) show a smooth surface compared with those of raw zeolite and iron-oxide-coated zeolite. This change in surface morphology is due to the polymerization of methacrylic acid onto the iron-oxide-coated zeolite.

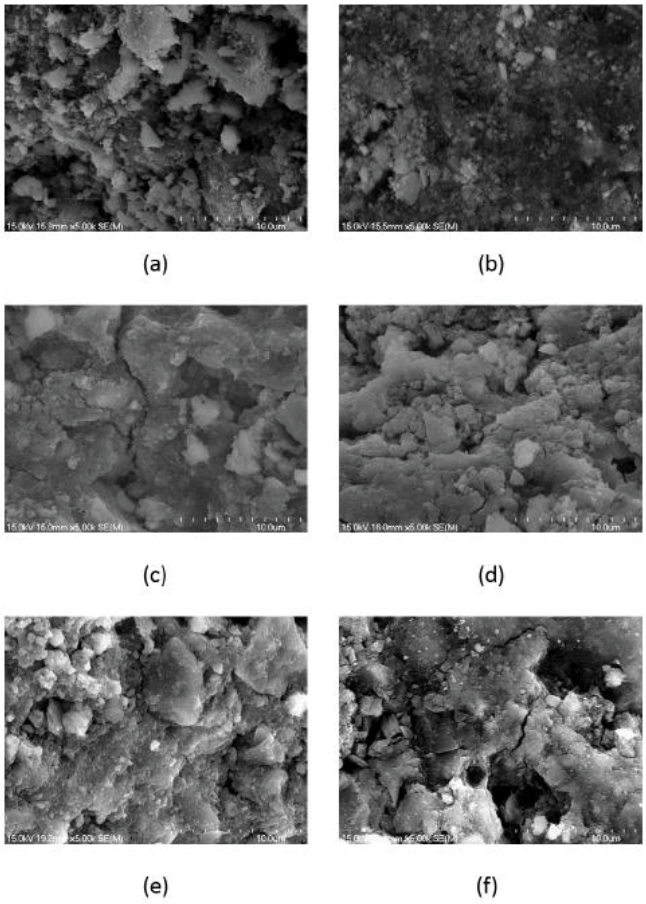

Fig. 3. SEM micrographs of (a) raw zeolite, (b) iron-oxide-coated zeolite, (c) MA-zeolite (15 min), (d), MA-zeolite (30 min), (e) MA-zeolite (60 min), and (f) MA-zeolite (120 min).

3.2. Adsorption of Fe(II), Mn(II), and As(III) for optimization of MA-zeolite

The adsorption of Fe(II), Mn(II), and As(III) by the modified zeolite was studied at room temperature (Table 1). The adsorption experiments were carried out using adsorbents prepared according to graft polymerization time from 15 to 120 min. The initial concentrations of Mn(II), Fe(II), and As(III) were 10, 10, and 1 mg/L, respectively.

Fig. 4(a) shows the adsorption rate for Fe(II) ions of MA-zeolite polymerized for 15, 30, 60, and 120 min.

Iron(II) is a charged solute at pH 3–4, which is the experimental condition of the solution. Comparing the MA-zeolite polymerized for 15, 30, 60, and 120 min, slightly better adsorption was observed for the zeolite polymerized for 15 min. The Fe(II) concentration of the solution treated with MA-zeolite (15 min) dramatically changed from 10 mg/L to around 0.21 mg/L over 30 min. Thus, the maximum removal percentage toward Fe(II) of MA-Zeolite (15 min) was 97.9%.

Fig. 4(b) shows the adsorption rates for Mn(II) ions removed by MA-zeolite polymerized for 15, 30, 60, and 120 min. The concentration of Mn(II) also changed from 10 to 0.5 mg/L over 30 min. All adsorbents showed similar adsorption efficiencies. The removal percentage for Mn(II) of all the adsorbents was about 95%.

The effect of polymerization time on the removal of arsenic(III) was studied at pH 3–4 at room temperature, as shown in Fig. 4(c). The adsorption efficiency of arsenic was remarkably lower than that of iron and manganese in the short-term experiments (within 30 min) because of the arsenic binding mechanism [20,21].

In this period, the arsenic(III) concentration fell from 1 to 0.95 mg/L, and there was no significant change in the removal of arsenic between different adsorbents. Thus, only small amounts of As(III) were removed (<10%) regardless of adsorbent. So, MA-zeolite (15 min) is considered as the optimum adsorbent and was used for further study.

Table 1
Summary of adsorption experiment conditions

Parameter	Operation condition
Experiment method	Batch type
Dose (g/L)	25
Temperature (°C)	25 ± 0.5
Initial pollutant concentration (mg/L)	Mn(II) 10
	Fe(II) 10
	As(III) 1
Solution volume (mL)	40
pH	3–4

3.3. Effect of adsorbent

The removal ratios (C/C_i) for Fe(II), Mn(II), and As(III) were determined using the adsorbents at room temperature and a contact time of 360 min at initial Fe(II), Mn(II), and As(III) concentrations of 10, 10, and 1 mg/L, respectively. The results are presented in Fig. 5. The experiments were carried out to investigate the influence of the surface character on metal adsorption.

Fig. 5(a) shows that the adsorption efficiency of Fe(II) increased when using the MA-zeolite (15 min). As shown in Fig. 5(a), Fe(II) adsorption by the iron-oxide-coated zeolite and MA-zeolite was high in the first 5 min of contact time. Initially, the removal efficiencies of unmodified zeolite, iron-oxide-coated zeolite, and MA-zeolite (15 min) were 47.1%, 98.7%, and 84.4%, respectively. With prolonged time, C/C_i decreased and reached a steady state. Then, 6 h later, 95.4%, 46.3%, and 99.1%, respectively, of the Fe(II) ions had been absorbed. In the case of iron-oxide-coated zeolite, the C/C_i of Fe(II) increased again. This is because the surface of the zeolite suffers from iron dissolution. MA-zeolite (15 min) showed the highest iron adsorption. Possibly, the carboxylic acid groups of the MA-zeolite increased the reactivity and the effectiveness for Fe(II) adsorption. As shown in Fig. 5(b), the adsorption efficiency of MA-zeolite for Mn(II) was higher than those of other adsorbents. The removal efficiency of manganese was different from that of iron. After 30 min reaction time, the removal efficiency of the raw zeolite, iron-oxide-coated zeolite, and MA-zeolite were 17%, 25%, and 94%, respectively.

The removal efficiency of MA-zeolite was 5.5 times higher than raw zeolite and 3.76 times higher than that of the iron-oxide-coated zeolite. The removal efficiency of MA-zeolite

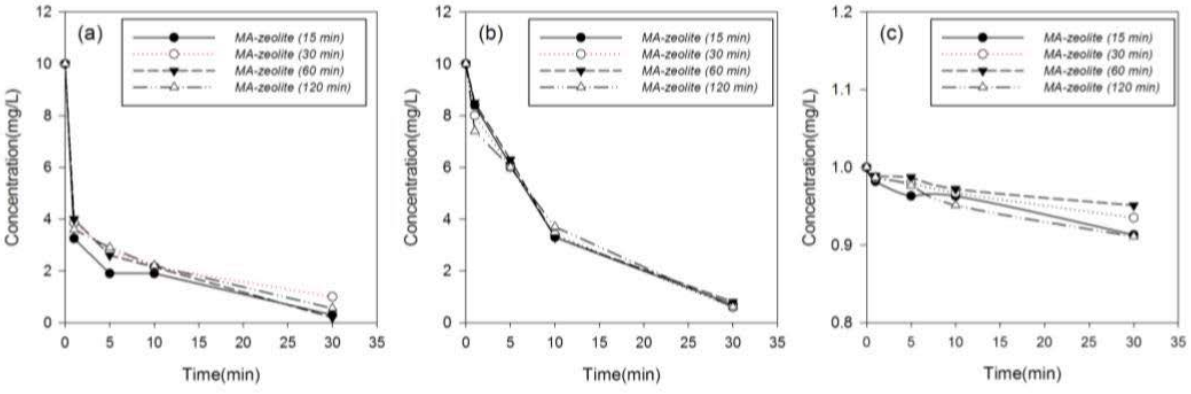

Fig. 4. Adsorption of (a) Fe(II), (b) Mn(II), and (c) As(III) by the zeolite modified by grafting polymerization.

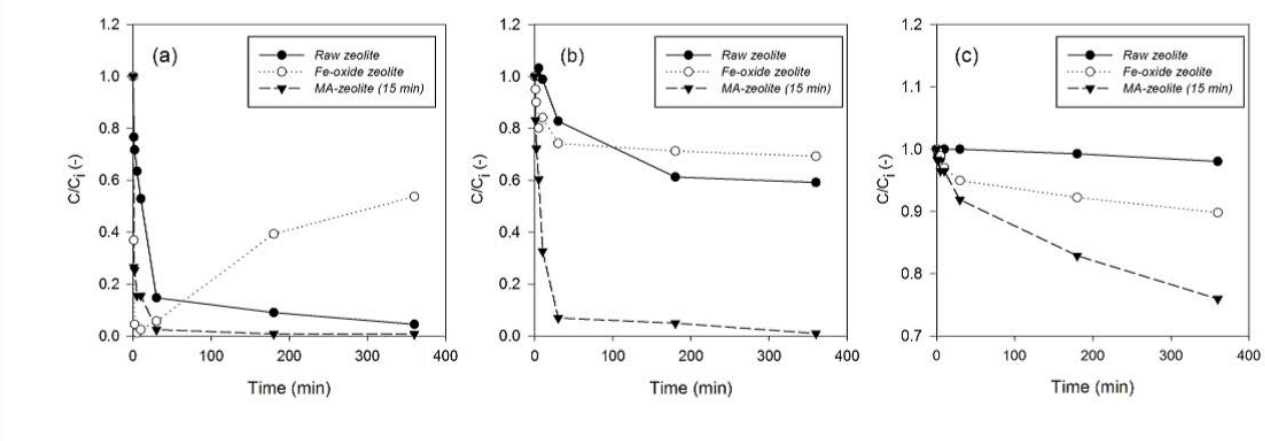

Fig. 5. Comparison of absorption of heavy metal ions by raw zeolite, iron-oxide-coated zeolite, and MA-zeolite (15 min): (a) Fe(II), (b) Mn(II), and (c) As(III) (C_i is the concentration of metal ions in the initial solution, and C is the concentration of metal ions in the final solution).

for manganese was very high because the modified carboxyl group on the surface facilitates adsorption of manganese. The negative charge of the surface induced by the carboxylic acid groups is suitable for removing the positively charged heavy metals [22].

The adsorption test results for arsenic are shown in Fig. 5(c). After 30 min, the removal efficiencies of raw zeolite, iron-oxide-coated zeolite, and MA-zeolite were 0.5%, 5%, and 9%, respectively. After 6 h reaction, the removal efficiencies of raw zeolite, iron-oxide-coated zeolite, and MA-zeolite were 2%, 9%, and 25%, respectively. MA-zeolite (15 min) had a removal efficiency of 25%, which is 2.5 times higher than those of raw zeolite and iron-oxide-coated zeolite.

When arsenic is present alone, it is positively charged. However, arsenic easily bonds with oxygen and hydrogen in water, forming negatively charged species. The adsorption efficiency is improved by coating iron oxide on the surface of zeolite, which acts as a cation exchange resin.

Based on the results in Fig. 5(b), the pseudo-first-order (PFO) and pseudo-second-order (PSO) models were fitted to the adsorption isotherms, and the adsorption constants obtained from these isotherms are given in Table 2. In this study, we adopted the PFO and PSO equation to calculate the adsorption capacity (q_e).

The PFO equation is shown in Table 2. The corresponding SigmaPlot equation included in the category "Exponential Rise to Maximum, Single, 2 Parameter" is $f = a(1 - e^{(-bx)})$. The corresponding parameters are $f = q_t$, $a = q_e$, and $b = k_1$. The PSO equation is also shown in Table 2. The corresponding SigmaPlot form included in the equation category "Exponential Rise to Maximum, Single, 2 Parameter" is $f = ax/(b + x)$. The corresponding parameters are $f = q_t$, $a = (k_2q_e)q_e$, and $b = 1/(k_2q_e)$.

The kinetic study is useful in predicting adsorption rate constants and expected adsorption capacity. The PFO and PSO kinetic models were investigated for three different adsorbents for Mn(II) adsorption at a temperature of 24°C. The nonlinear forms of the PFO and PSO contain the following variables: q_e is the adsorption capacity of Mn(II) per unit weight of adsorbent at equilibrium and at time t (min), and k_1 and k_2 are the PFO and PSO rate constants, respectively. The values of k_1 and k_2 and q_e were determined from the slope and intercept in the graph of q_t versus t (Fig. 6) for different Mn(II) adsorbents and are listed in Table 2. From the data in Table 2, the calculated q_e value in the PSO model is similar to the experimental value with a high correlation coefficient. On the other hand, the q_e calculated from the PFO model showed less agreement than the data obtained for the PSO kinetic model. Thus, the kinetics of the adsorption of Mn(II) onto zeolite adsorbents can be explained adequately by the PSO kinetic model.

4. Conclusions

In this study, zeolite modified by polymerization with methacrylic acid was used as an adsorbent for the removal of

Table 2
Comparison of kinetic parameters for the adsorption of Mn(II) by raw zeolite, iron-oxide-coated zeolite, and MA-zeolite (15 min)

Sample	Pseudo-first-order model $q_t = q_e\left(1-e^{-k_1t}\right)$			Pseudo-second-order model $q_t = k_2q_e^2t/1 + k_2q_et$		
	$q_{e,\exp}$ (mg/g)	$q_{e,\mathrm{cal}}$ (mg/g)	R^2	$q_{e,\exp}$ (mg/g)	$q_{e,\mathrm{cal}}$ (mg/g)	R^2
Raw zeolite	4.5	4.43	0.94	4.5	4.59	0.95
Fe-oxide-coated zeolite	3.1	2.79	0.91	3.1	2.95	0.95
MA-zeolite	10	9.72	0.99	10	10.29	0.99

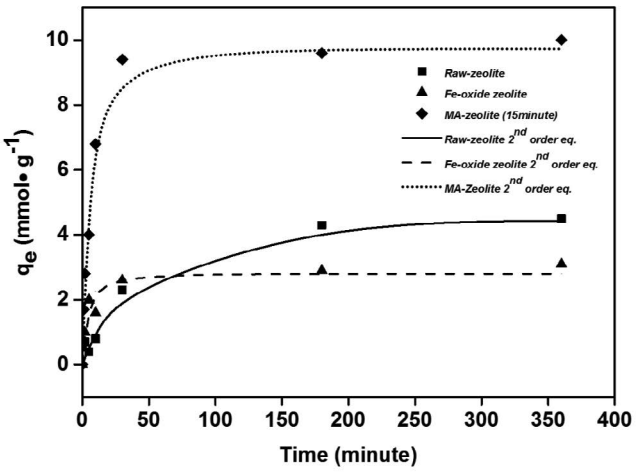

Fig. 6. Mn(II) uptake during adsorption onto raw zeolite, iron-oxide-coated zeolite, and MA-zeolite (15 min) with pseudo-second-order kinetic model fitting.

iron(II), manganese(II), and arsenic(III) from the water. The BET surface area and SEM and FTIR analyses confirm the characteristics of the graft polymerized zeolite, which had a high removal efficiency for iron, manganese, and arsenic from aqueous solution. The graft polymerization resulted in a negative charge on the surface that improved the efficiency of heavy metal adsorption. Because arsenic was removed by conventional arsenic adsorption mechanisms, further work on this method is needed.

Acknowledgment

This research was supported by a grant (17CTAP-C133297-01) from the Infrastructure and Transportation Technology Promotion Research program funded by the Ministry of Land, Infrastructure, and Transport of the Korean government.

References

[1] R. Costanza, R. D'Arge, The value of the world's ecosystem services and natural capital, Nature, 387 (1997) 253.
[2] P. Roccaro, C. Barone, G. Mancini, F.G.A. Vagliasindi, Removal of manganese from water supplies intended for human consumption: a case study, Desalination, 210 (2007) 205–214.
[3] D. Ellis, C. Bouchard, G. Lantagne, Removal of iron and manganese from groundwater by oxidation and microfiltration, Desalination, 130 (2000) 255–264.
[4] A. Alpatova, S. Verbych, M. Bryk, R. Nigmatullin, N. Hilal, Ultrafiltration of water containing natural organic matter: heavy metal removing in the hybrid complexation-ultrafiltration process, Sep. Purif. Technol., 40 (2004) 155–162.
[5] B.A.M. Al-Rashdi, D.J. Johnson, N. Hilal, Removal of heavy metal ions by nanofiltration, Desalination, 315 (2013) 2–17.
[6] S. Wang, Y. Peng, Natural zeolites as effective adsorbents in water and wastewater treatment, Chem. Eng. J., 156 (2010) 11–24.
[7] W. Zou, H. Bai, L. Zhao, K. Li, R. Han, Characterization and properties of zeolite as an adsorbent for removal of uranium (VI) from solution in fixed bed column, J. Radioanal. Nucl. Chem., 288 (2011) 779–788.
[8] K. Margeta, N. Zabukovec, M. Siljeg, A. Farkas, Natural zeolites in water treatment: How effective is their use?, W. Elshorbagy, Ed., Water Treatment, InTechOpen, 2013, pp. 81–112.
[9] B. Calvo, L. Canoira, F. Morante, J.M. Martínez-Bedia, C. Vinagre, J.E. García-González, J. Elsen, R. Alcantara, Continuous elimination of Pb^{2+}, Cu^{2+}, Zn^{2+}, H^+ and NH_4^+ from acidic waters by ionic exchange on natural zeolites, J. Hazard. Mater., 166 (2009) 619–627.
[10] D. Barloková, J. Ilavský, Removal of iron and manganese from water using filtration by natural materials, Pol. J. Environ. Stud., 19 (2010) 1117–1122.
[11] F.L. Fu, Q. Wang, Removal of heavy metal ions from wastewaters: a review, J. Environ. Manage., 92 (2011) 407–418.
[12] R. Roque, J. De Onate, E. Reguera, E. Navarro, Pyrrole oligomerization in a zeolite, J. Mater. Sci. Lett., 12 (1993) 1037.
[13] N. Densakulprasert, L. Wannatong, D. Chotpattananont, Electrical conductivity of polyaniline/zeolite composites and synergetic interaction with CO, Mater. Sci. Eng. B., 117 (2005) 276–282.
[14] Y.H. Shin, W.D. Lee, S.S. Im, Effect of A-zeolite on the crystallization behavior of in-situ polymerized poly (ethylene terephthalate) (PET) nanocomposites, Macromol. Res., 15 (2007) 662–670.
[15] Š. Cerjan Stefanović, N. Zabukovec Logar, K. Margeta, N. Novak Tušar, I. Arčon, K. Maver, J. Kovač. V. Kaučič, Structural investigation of Zn^{2+} sorption on clinoptilolite tuff from the Vranjska Banja deposit in Serbia, Microporous Mesoporous Mater., 105 (2007) 251–259.
[16] S. Karimi, J. Feizy, F. Mehrjo, M. Farrokhnia, Detection and quantification of food colorant adulteration in saffron samples using chemometric analysis of FT-IR spectra, RSC Adv., 6 (2016) 23085–23093.
[17] P. Ino, M. Nanodelcev, A. Drmota, A mechanism for the adsorption of carboxylic acids onto the surface of magnetic nanoparticles, Mater. Technol., 42 (2008) 79–83.
[18] R. Baran, Y. Millot, T. Onfroy, J.M. Krafft, S. Dzwigaj, Influence of the nitric acid treatment on Al removal, framework composition and acidity of BEA zeolite investigated by XRD, FTIR and NMR, Microporous Mesoporous Mater., 163 (2012) 122–130.
[19] J. Grzybek, B. Gil, W.J. Roth, M. Skoczek, A. Kowalczyk, L. Chmielarz, Characterization of Co and Fe-MCM-56 catalysts for NH_3-SCR and N_2O decomposition: an in situ FTIR study, Spectrochim. Acta, Part A, 196 (2018) 281–288.
[20] E. Erdem, N. Karapinar, R. Donat, The removal of heavy metal cations by natural zeolites, J. Colloid Interface Sci., 280 (2004) 309–314.
[21] O.S. Thirunavukkarasu, T. Viraraghavan, K.S. Subramanian, Arsenic removal from drinking water using iron oxide-coated sand, Water, Air, Soil Pollut., 142 (2003) 95–111.
[22] P.A. Brown, S.A. Gill, S.J. Allen, Metal removal from wastewater using peat, Water Res., 34 (2000) 95–111.